# Deflection of Global Ion Flow by the Martian Crustal Magnetic Fields

Kai Fan[1,2,3] , Markus Fraenz[4] , Yong Wei[1,2,3] , Jun Cui[5,6] , Zhaojin Rong[1,2,3] , Lihui Chai[1,2,3] , and Eduard Dubinin[4]

[1] Key Laboratory of Earth and Planetary Physics, Institute of Geology and Geophysics, Chinese Academy of Sciences, Beijing, People's Republic of China
[2] College of Earth and Planetary Sciences, University of Chinese Academy of Sciences, Beijing, People's Republic of China
[3] Beijing National Observatory of Space Environment, Institute of Geology and Geophysics, Chinese Academy of Sciences, Beijing, People's Republic of China
[4] Max-Planck-Institute for Solar System Research, Goettingen, Germany; fraenz@mps.mpg.de
[5] Sun Yat-Sen University, School of Atmospheric Sciences, Zhuhai, People's Republic of China
[6] Key Laboratory of Lunar and Deep Space Exploration, National Astronomical Observatories, Chinese Academy of Sciences, Beijing, People's Republic of China

## Abstract

Without the protection of a global magnetic field, erosion of the Martian ionosphere by the solar wind leads to abundant loss of atmospheric particles. Although the crustal magnetic fields in the Martian southern hemisphere are strong enough to affect the dayside-induced magnetosphere, there is still limited evidence for the deflection of the solar winds by the crustal magnetic fields. With 4 years of ion data measured by the Mars Atmosphere and Volatile EvolutioN mission, we investigate the flow pattern of protons, $O^+$, and $O_2^+$ when the crustal fields rotate to different local times. Our result is the first evidence that suggests the crustal magnetic fields can withstand the solar wind flows on the Martian dayside and can effectively trap heavy ions below 1000 km. The gyroradii of heavy ions in the strong crustal fields regions are one order of magnitude smaller than in other regions. The trapping effect causes different flow patterns, while the crustal fields rotate to different subsolar regions but are attenuated at higher altitudes. Observations provide essential information to investigate the effect of the crustal magnetic fields on heavy-ion flows and understand the role of the crustal magnetic fields in the interaction between the solar wind and the Martian atmosphere.

## 1. Introduction

Global magnetic fields, such as the Earth's, deflect the dayside solar wind and reduce the escape rates of planetary ions (e.g., Moore & Horwitz 2007; Wei et al. 2012). In contrast, Mars is unprotected by a similar magnetic field; its ionospheric particles are directly exposed to the impinging solar wind and consequently accelerated by the solar wind electric fields (e.g., Russell et al. 1990; Brain et al. 2002; Dubinin et al. 2011; Dong et al. 2015). Such a process is generally considered as an important channel through which Mars has lost most of its atmosphere and surface water over geological timescales (e.g., Barabash et al. 2007; Jakosky et al. 2015a). The global picture of the solar wind interactions with Mars is complicated by the presence of crustal magnetic fields, an issue that has been investigated extensively by numerical simulations (e.g., Harnett & Winglee 2007; Ma et al. 2014; Fang et al. 2015), but has not been fully supported by existing observations yet due to the lack of simultaneous magnetic field and ion flow measurements in the near-Mars environment.

The Martian crustal magnetic fields were first discovered by the Mars Global Surveyor in 1998 and known to cluster over the southern hemisphere of the planet (Acuña et al. 1998; Connerney et al. 2005). A remarkable impact of such magnetic fields on the dayside Martian ionosphere has been revealed by numerous works with the aid of radio occultation (e.g., Ness et al. 2000; Withers et al. 2005), radar sounding (e.g., Duru et al. 2006; Andrews et al. 2015), Langmuir probe (e.g., Flynn et al. 2017), and mass spectrometer measurements (e.g., Withers et al. 2019; Wu et al. 2019), manifesting as a clear enhancement near the strong crustal magnetic fields and interpreted as a natural outcome of field-aligned plasma transport (e.g., Matta et al. 2015). This is to be distinguished from the nightside where the effect of the strong magnetic fields manifests as substantially reduced ionospheric plasma content due to the shielding of the solar wind electrons precipitation by closed magnetic loops preferentially occurring near the strong crustal magnetic anomalies (e.g., Lillis et al. 2010, 2018). The configuration of crustal magnetic fields also controls suprathermal electron angular distributions (e.g., Mitchell et al. 2001; Brain et al. 2007; Xu et al. 2017) and the intrusion depth of the solar wind electrons (e.g., Fränz et al. 2006b; Dubinin et al. 2008; Niu et al. 2020).

By contrast, the effects of the crustal magnetic fields on ionospheric heavy ions are still under debate. Crider et al. (2004) showed that the crustal fields can push up the magnetic pileup boundary and photoelectron boundary. Due to the small Martian radius and the weak Martian gravity, accelerated heavy ions escape from Mars within several cyclotron periods (e.g., Lundin et al. 1989, 2011; Brain et al. 2015). Observations from the Analyzer of Space Plasma and Energetic Atoms (ASPERA-3) on board the Mars Express found an asymmetry in total fluxes of heavy ions between the areographic north and south (Nilsson et al. 2006, 2011; Dubinin et al. 2012). However, the differences of the total ion-loss rates measured from the Martian tail between two hemispheres are not distinctive, raising questions about the efficacy of the crustal fields' shielding effect (Ramstad et al. 2016). Several numerical simulations (e.g., Ma et al. 2002, 2004; Harnett & Winglee 2005; Ma & Nagy 2007) suggest that the crustal magnetic field may form a mini-magnetosphere to trap heavy ions and deflect the solar wind flow on the Martian dayside. However, this feature has not been systematically observed in the data. The Mars Atmosphere and Volatile EvolutioN (MAVEN) spacecraft provides a comprehensive set of plasma instruments, which allows us to observe the magnetic fields and ion flow simultaneously for the first time (Jakosky et al. 2015b). This is an excellent chance to

investigate the effects of the crustal magnetic fields on interactions between the solar wind and the heavy Martian ions.

## 2. Data

MAVEN carries two electrostatic analyzers to measure the solar wind protons and planetary ions independently. The solar wind Ion Analyzer (SWIA) does not discriminate between ion species but has a high spatial resolution (4°.5 in the solar wind direction) for protons from 25 eV to 25 keV. SWIA provides ion moment data such as density, velocity, temperature, vector heat flux, and pressure tensor (Halekas et al. 2015). Heavy ions are measured by the Supra Thermal And Thermal Ion Composition (STATIC) instrument. STATIC provides ion data in the energy range of 0.1 eV–30 keV, distinguishing ion species such as $H^+$, $He^+$, $O^+$, $O_2^+$, and $CO_2^+$ (McFadden et al. 2015). STATIC has three different modes (Ram, Conic, and Pick-up), which provide data with different time, energy, and spatial resolution. Here we used the ion density and velocity calculated from 32 energy steps, 8 mass steps, 4 deflector angles, 16 azimuth angles with a 4 s time resolution. A total of 4 years of ion data are used in this work covering the period from 2014 October to 2018 November (a total of 6161 orbits). STATIC data were corrected for the influence of the spacecraft potential and spacecraft speed. Velocities are calculated in the Mars-centered Solar Orbital (MSO) coordinate and then transformed to planet-fixed coordinates (i.e., IAU Mars). In the right-handed MSO coordinate, the $x$-axis is defined as the direction of the vector from which points the center of Mars points to the Sun; the $z$-axis is perpendicular to the plane of Mars' heliocentric orbit and points northward, and the $y$-axis completes the right-hand system. This work also used magnetic field data measured by the magnetometer on board the MAVEN spacecraft to compute the ion local gyroradius (Connerney et al. 2015a). The magnetometer provides accurate magnetic field observations on both strong and weak parts of the crustal magnetic fields (Connerney et al. 2015b).

## 3. Results

On the Martian dayside, an induced magnetosphere boundary (IMB) is formed between heavy planetary ions and the solar wind flows (e.g., Luhmann et al. 1992). In the subsolar region, the shocked solar wind flows are deflected by the induced magnetosphere and in the first approximation follow the gas-dynamic flow around a sphere. The IMB in the northern hemisphere is highly compressed by the solar wind and lower than 500 km on average (e.g., Edberg et al. 2009; Matsunaga et al. 2017). In contrast, as Figure 1 shows, in the regions above the strong crustal fields at 550 km altitude, most of the solar wind protons are stopped from entry into crustal fields (see Figures 1(a) and (b)) and heavy ions such as $O^+$ and $O_2^+$ are trapped (see Figures 1(c)–(f)). The three different species' total fluxes show a hemispheric asymmetry oriented along with the outlines of the crustal magnetic fields in the areographical map. Some flow vortices are visible in the streamline plots located close to the strongest sources of the crustal magnetic field. The radius of vortex is larger in the $O_2^+$ flows than in $O^+$. This indicates that the crustal magnetic fields' control depends on the ion's gyroradius. Here it is noted that Figure 1 contains 4 years of statistics, thereby smoothing out the effect of external factors on the flow pattern, e.g., the interplanetary magnetic field, solar wind dynamic pressure, and

the variations of solar extreme ultraviolet radiation. Ions measured by SWIA also show similar features for $H^+$ ions as measured by STATIC (see Figure 1(g)), which consistently demonstrates the effect of the crustal magnetic fields on the deflection of the solar wind flows.

The magnitudes of the crustal magnetic fields decrease with increasing altitude. In Figure 2, at 650 km, the weaker part of the crustal field in the regions at 50°E and 300°E near the equator are no longer able to resist the solar wind's pressure. Only the strong crustal fields region between 150°E and 250°E on the southern hemisphere effectively deflect the solar wind flows at this altitude. This shielding effect of the localized crustal fields reaches its limit at even higher altitudes; there the size of the lower fluxes region shrinks, and the flow streamlines are dominated by the shocked solar winds. Results from Figures 1 and 2 are highly consistent with the crustal magnetic fields' topology published by Xu et al. (2017), who statistically investigate the occurrence rates of closed, draped, and open field lines by distinguishing the solar wind electrons from the ionospheric electrons. The observations suggest for altitudes above 400 km that the closed field lines in the south and the draped field lines in the north form an environment of hemispheric asymmetry. Moreover, the averaged streamlines of different ion species support the crustal magnetic fields that have a substantial effect on the deflection of the solar wind flows and on the trapping of heavy ions.

## 4. Discussion

Fan et al. (2019) already investigated thermal $O^+$ ions (energy >30 eV) below 600 km and discovered the lower flux region above the strong crustal magnetic fields. The current work traces the solar wind protons and planetary heavy ions in the dayside IMB regions and reveals significant deflection of the solar wind flow and trapping of heavy ions by the crustal magnetic fields. Several simulations have previously been conducted to investigate the effect of the crustal magnetic fields on plasma flows near Mars. The model by Harnett & Winglee (2007) suggests that the strong crustal fields not only prevent the solar wind flows from the entrance but also protect the cold, dense plasma up to 1000 km altitude in the southern hemisphere. This causes a hemispheric asymmetry in plasma fluxes, as we observed in Figures 1 and 2. The same phenomena are also found in previous observations from the Mars Express and MAVEN spacecraft (Fränz et al. 2006a; Dubinin et al. 2019). Our results are also consistent with the three-dimensional multispecies MHD model by Ma et al. (2002, 2004), which suggests that the crustal fields raise the altitude of the topside ionosphere in the southern hemisphere, which leads to an enhancement in ion densities observed between 250 and 600 km altitude on the Martian dayside. In Figure 3, we demonstrate the altitude dependency of the crustal field trapping effect on $O^+$ ions, while the strongest crustal fields (i.e., those centered at 180° east longitude) rotate to the noon side (local time from 9 to 15 hr). In Figures 3(c) and (e), the gyroradius of $O^+$ ions increase with altitude and decrease with the magnitude of the crustal field. By contrast, in Figures 3(d) and (e), the total fluxes of $O^+$ ions increase with the strength of the crustal fields. Gyroradii have been calculated from the local velocity and local magnetic fields. As Figure 3(e) shows, the local gyroradii of the $O^+$ ions above the strong crustal magnetic fields region are one order of magnitude smaller than above weak crustal fields at 550 km.
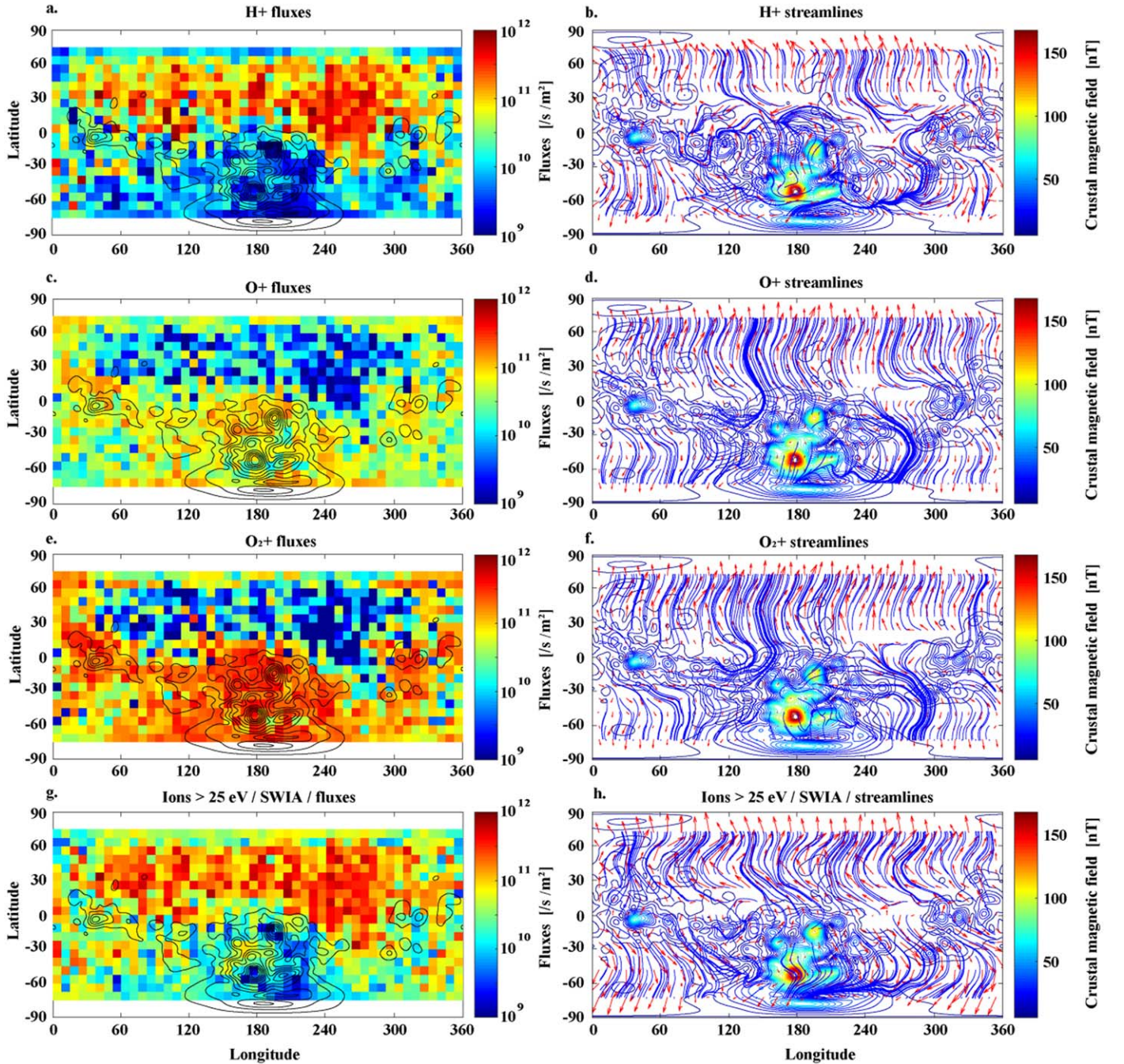
**Figure 1.** Maps of average fluxes (left column) and streamlines (right column) of different ion species ($H^+$, $O^+$, $O_2^+$, total ions measured by SWIA) in areographical coordinates for local times from 9 to 15 hr, from 4 years of data. The black contours in the left column are outlines of the crustal magnetic fields at 400 km given by the Cain model (Cain et al. 2003). The color indicates total fluxes (left column) and magnitudes of the crustal magnetic fields (right column), respectively. Red arrows in the streamline panels give the median value of the velocities' horizontal component within each longitude–latitude cell.

Results in Figure 3(a) also suggest the strong dependency of gyroradii on the magnitude of the crustal magnetic fields. Additionally, above the strong crustal magnetic fields at 550 km, the closed magnetic field lines are dominating the magnetic field configuration based on observations made by the SWEA instrument (Xu et al. 2017; Weber et al. 2019). Our results confirm that the strong crustal magnetic fields stand off the solar wind flows on the Martian dayside, exactly as predicted by the simulation in Ma et al. (2014).

The deflection of ion flows by the strong crustal fields also appears in the streamline patterns at the terminator. The global hydrodynamic flows may overcome the crustal fields at the terminator, but at altitudes as low as 550 km, $O^+$ and $O_2^+$ flows in the magnetosphere are obstructed by the crustal magnetic fields and make a "detour" around the field structures. In Figures 4(a) and (d), the westward flows on the dawn side (local time from 3 to 9 hr) are stopped by the crustal magnetic fields at 200°E. In Figures 4(b) and (e), on the dusk side (local
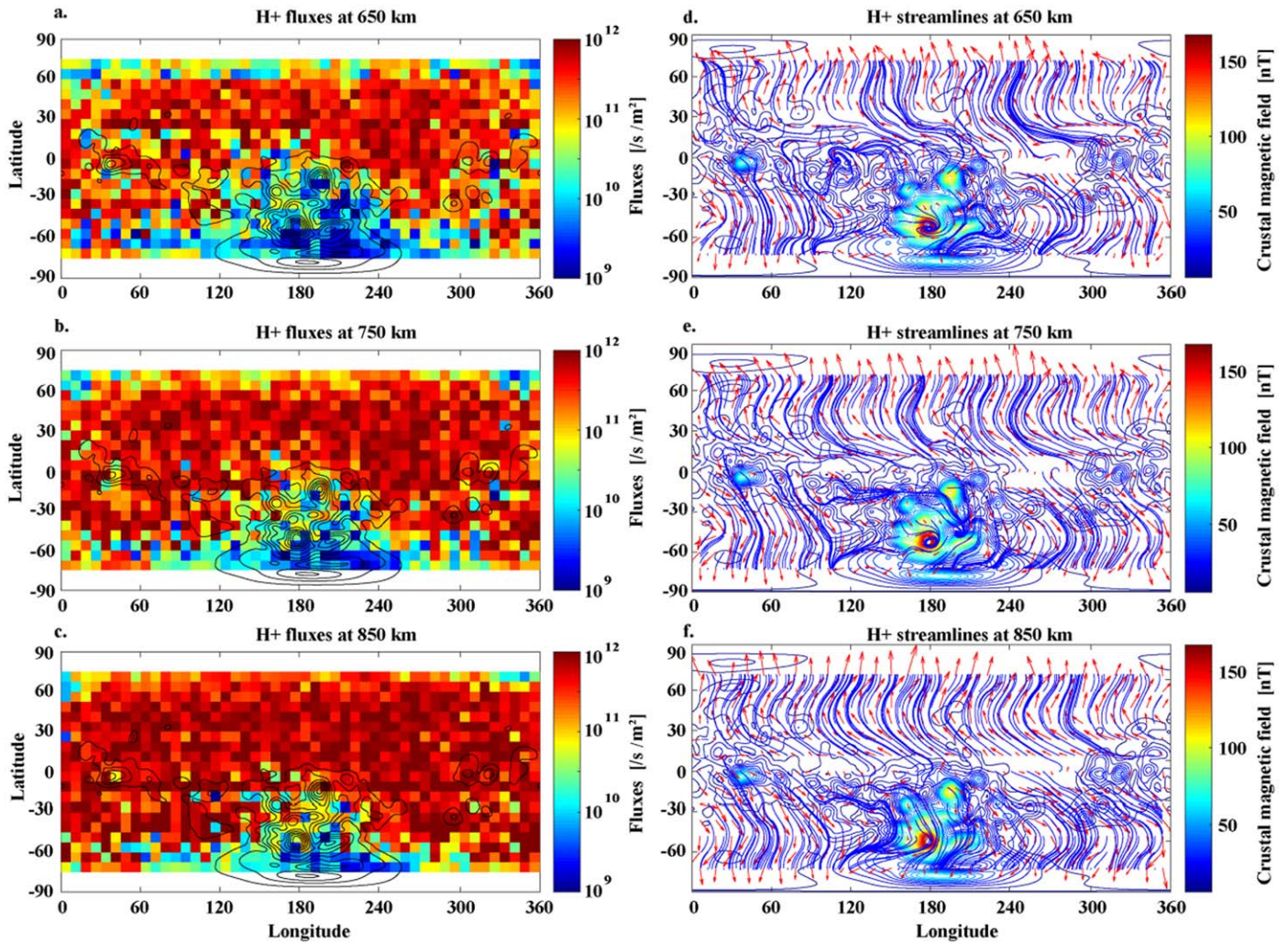
**Figure 2.** Images are in the same format as Figure 1. Fluxes and streamlines of H$^+$ ions are measured by STATIC. From top to bottom, data are for altitudes 650 km, 750 km, and 850 km, respectively.

time from 15 to 21 hr), flows of heavy ions are eastward and streamlines on the southern hemisphere are converging at the east side of the strong crustal fields (150°E). Similar to Figure 3(a), the gyroradii of O$^+$ and O$_2^+$ ions above the crustal magnetic field region in Figures 4(c) and (f) are also nearly one order less than outside of these regions. We suggest that the crustal magnetic fields are critical in trapping heavy ions. Models from Harnett & Winglee (2005) discussed the flow patterns of plasma while the crustal fields are rotating to different subsolar regions. Simulations from the latest MHD models also suggest that the crustal magnetic fields control the cross-section area at the terminator and affect the global loss rates (Fang et al. 2017). The detailed relationship between the crustal magnetic fields and dawn–dusk asymmetry will be investigated in future studies.

The strong crustal fields can trap the local heavy ions. However, this does not necessarily lead to significant changes in total loss rates. The total escape rates of planetary ions observed in the Martian tail did not show a significant dependence on the synchronous location of the crustal fields; the escape rate from the southern hemisphere is 46% $\pm$ 18% of the global rate based on 8 years of observations made by Mars Express (Ramstad et al. 2016). Results from the MHD

simulations (e.g., Ma et al. 2014, 2015; Fang et al. 2015) also suggest the global escape rates are not sensitive to the rotation of the crustal magnetic fields. The global escape rate from the southern hemisphere is 50% less than from the northern hemisphere while the crustal fields are located at dawn and noon, but the escape rate from the two hemispheres are about the same while the crustal fields are at dusk and midnight, which is also consistent with former model simulations (e.g., Ma & Nagy 2007; Fang et al. 2010).

The total ion loss is not determined in our work; one important reason for this is that the altitudes discussed in this work are too low to determine the ultimate fate of the heavy ions. Another reason is the directions of ion flows measured by STATIC below 1000 km were nearly horizontal, as Figure 3(b) shows. But the escaping fluxes are determined by the vertical flows. The bias in observations limits a more in-depth analysis in evaluating the geographical distribution of outward fluxes (e.g., Brain et al. 2015) but will not affect the crustal fields' trapping effect on horizontal flows, which we discussed above. Based on the flow patterns we discussed in this work, one possible reason that the crustal magnetic field did not strongly affect the global ion-loss rates is the strong trapping effect, which isolates the interactions between plasma inside the
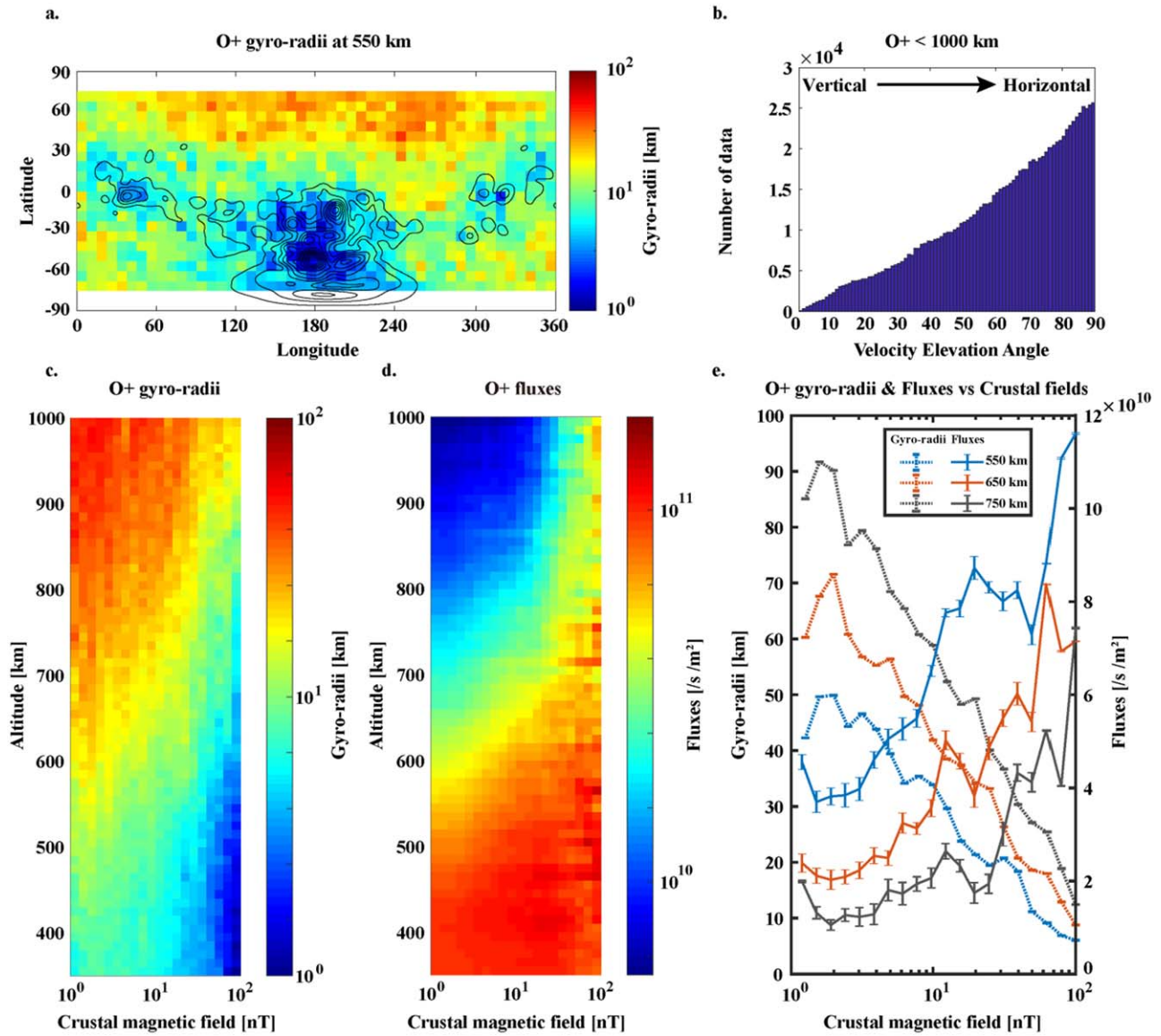
**Figure 3.** (a) Map of dayside O$^+$ ions' gyroradii at 550 km altitude. Black contours indicate the outlines of the crustal fields at 400 km given by the Cain model. (b) Distribution of velocity elevation angles, 0° indicate vertical flows, and 90° indicate horizontal flows. (c) and (d) Gyroradii and fluxes of O$^+$ ions vs. altitude and magnitude of the crustal magnetic fields. (e) Profiles of O$^+$ ions' gyroradii and fluxes vs. the crustal magnetic fields at 550 km, 650 km, and 750 km, respectively.

crustal magnetic fields and the outside flows. That is, the strong crustal magnetic field might not only prevent heavy ions inside the strong crustal fields from moving outward but also might prevent outside flows from entering. Hara et al. (2018) revealed that the crustal fields have a strong shielding effect by prohibiting the penetration of pick-up ions. The crustal magnetic fields seem to form a mini-magnetosphere to deflect outside heavy-ion flows.

## 5. Conclusions

The crustal magnetic fields in the Martian southern hemisphere expand the cold, dense ionosphere to higher altitudes and trap heavy ions. The former process leads to a larger contact area with the shocked solar wind, which can cause a higher ion loss, while the latter indicates an effect of shielding and therefore a protection of heavy ions from escape. This study for the first time shows the crustal fields' deflecting effect

on the dayside solar wind flow. Additionally, when the crustal magnetic fields rotate across the terminator, the fields may also prevent heavy ions such as O$^+$ and O$_2^+$ from flowing in the opposite direction. The local gyroradii of heavy ions in the strong crustal field region is at least one order smaller than that in other regions, which demonstrates the strong trapping effect of the crustal fields on heavy ions at lower altitudes. After all, the crustal magnetic fields significantly affect the interaction between the solar wind and the Martian ionospheric ions. As the illustration in Figure 5 shows, while the strongest crustal fields (black shell) rotate to different locations such as the dawn, dusk, or the subsolar sides, they are causing a deflection of the solar wind flows (red arrow). The strongest crustal magnetic fields act like a "shell" separating outside and inside plasma below 1000 km altitude. The crustal magnetic fields may have a considerable influence on the evolution history of the Martian atmosphere.
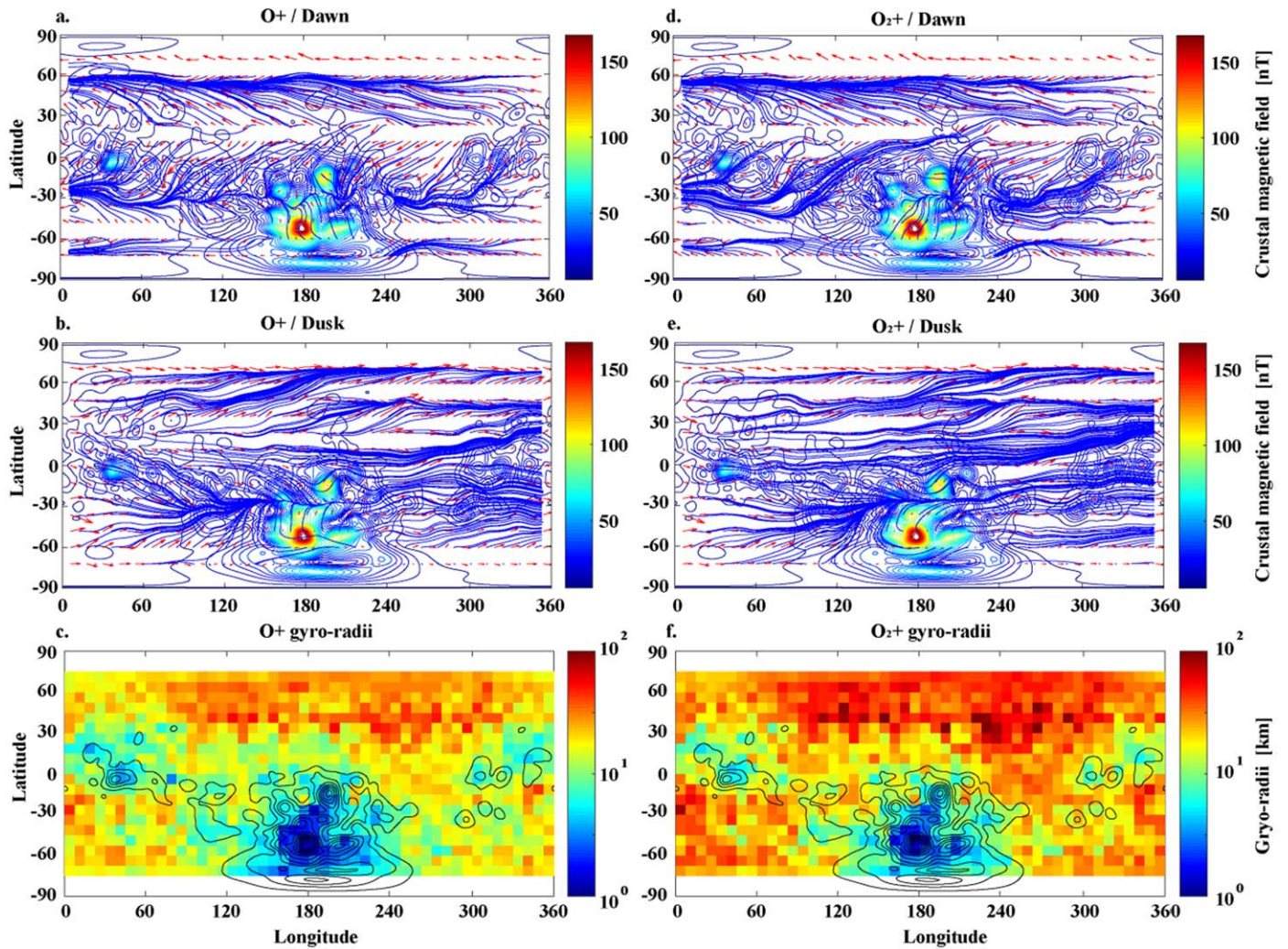
## Patterns of Terminator at 550 km



**Figure 4.** Streamlines and gyroradii of $O^+$ (left column) and $O_2^+$ (right column) measured by STATIC in a geographical map for local time at dawn (from 3 to 9 hr) and dusk (from 15 to 21 hr). The black contour in the left column shows outlines of the crustal fields. Color in the streamline panels indicates the magnitude of the crustal magnetic fields given by the Cain model. Color in the bottom row shows gyroradii of $O^+$ and $O_2^+$ ions.
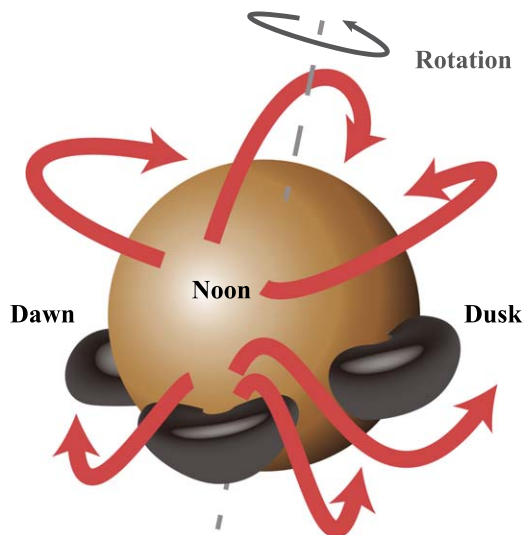


**Figure 5.** Illustration showing the deflection of ion flows by the crustal magnetic fields. Red arrows show the paths of the ion flows. Black shells on the southern hemisphere indicate the crustal magnetic fields (not to scale).

### ORCID iDs

Kai Fan https://orcid.org/0000-0003-2572-1587
Markus Fraenz https://orcid.org/0000-0003-4521-2931
Yong Wei https://orcid.org/0000-0001-7183-0229
Jun Cui https://orcid.org/0000-0002-4721-8184
Zhaojin Rong https://orcid.org/0000-0003-4609-4519
Lihui Chai https://orcid.org/0000-0001-8844-9176

# References

Acuña, M. H., Connerney, J. E. P., Wasilewski, P., et al. 1998, Sci, 279, 1676
Andrews, D. J., Edberg, N. J. T., Eriksson, A. I., et al. 2015, JGRA, 120, 3042
Barabash, S., Fedorov, A., Lundin, R., & Sauvaud, J.-A. 2007, Sci, 315, 501
Brain, D. A., Bagenal, F., Acuña, M. H., et al. 2002, JGRA, 107, 1428
Brain, D. A., Lillis, R. J., Mitchell, D. L., Halekas, J. S., & Lin, R. P. 2007, JGRA, 112, A09201
Brain, D. A., McFadden, J. P., Halekas, J. S., et al. 2015, GeoRL, 42, 9142
Cain, J. C., Ferguson, B. B., & Mozzoni, D. 2003, JGRE, 108, 5008
Connerney, J. E. P., Acuña, M. H., Ness, N. F., et al. 2005, PNAS, 102, 14970
Connerney, J. E. P., Espley, J., Lawton, P., et al. 2015a, SSRv, 195, 257
Connerney, J. E. P., Espley, J. R., DiBraccio, G. A., et al. 2015b, GeoRL, 42, 8819
Crider, D. H., Brain, D. A., Acuña, M. H., et al. 2004, SSRv, 111, 203
Dong, Y., Fang, X., Brain, D. A., et al. 2015, GeoRL, 42, 8942
Dubinin, E., Fraenz, M., Fedorov, A., et al. 2011, SSRv, 162, 173
Dubinin, E., Fraenz, M., Pätzold, M., et al. 2019, JGRA, 124, 9725
Dubinin, E., Fraenz, M., Woch, J., et al. 2008, P&SS, 56, 846
Dubinin, E., Fraenz, M., Woch, J., et al. 2012, EP&S, 64, 113
Duru, F., Gurnett, D. A., Averkamp, T. F., et al. 2006, JGRA, 111, A12204
Edberg, N. J. T., Brain, D. A., Lester, M., et al. 2009, AnGeo, 27, 3537
Fan, K., Fraenz, M., Wei, Y., et al. 2019, GeoRL, 46, 11764
Fang, X., Liemohn, M. W., Nagy, A. F., Luhmann, J. G., & Ma, Y. 2010, Icar, 206, 130
Fang, X., Ma, Y., Brain, D., Dong, Y., & Lillis, R. 2015, JGRA, 120, 10926
Fang, X., Ma, Y., Masanuga, K., et al. 2017, JGRA, 122, 4117
Flynn, C. L., Vogt, M. F., Withers, P., et al. 2017, GeoRL, 44, 10812
Fränz, M., Dubinin, E., Roussos, E., et al. 2006a, SSRv, 126, 165
Fränz, M., Winningham, J. D., Dubinin, E., et al. 2006b, Icar, 182, 406
Halekas, J. S., Taylor, E. R., Dalton, G., et al. 2015, SSRv, 195, 125
Hara, T., Luhmann, J. G., Leblanc, F., et al. 2018, JGRA, 123, 8572
Harnett, E. M., & Winglee, R. M. 2005, JGRA, 110, A07226
Harnett, E. M., & Winglee, R. M. 2007, JGRA, 112, A05207
Jakosky, B. M., Grebowsky, J. M., Luhmann, J. G., et al. 2015a, Sci, 350, aad0210
Jakosky, B. M., Lin, R. P., Grebowsky, J. M., et al. 2015b, SSRv, 195, 3
Lillis, R. J., Brain, D. A., England, S. L., et al. 2010, JGRA, 115, A11314
Lillis, R. J., Halekas, J. S., Fillingim, M. O., et al. 2018, JGRE, 123, 67
Luhmann, J. G., Russell, C. T., Brace, L. H., & Vaisberg, O. L. 1992, Mars (Tucson, AZ: Univ. Arizona Press), 1090
Lundin, R., Barabash, S., Yamauchi, M., Nilsson, H., & Brain, D. 2011, GeoRL, 38, L02102
Lundin, R., Zakharov, A., Pellinen, R., et al. 1989, Natur, 341, 609
Ma, Y., Fang, X., Russell, C. T., et al. 2014, GeoRL, 41, 6563
Ma, Y., Nagy, A. F., Hansen, K. C., et al. 2002, JGRA, 107, 1282
Ma, Y., Nagy, A. F., Sokolov, I. V., & Hansen, K. C. 2004, JGRA, 109, A07211
Ma, Y.-J., & Nagy, A. F. 2007, GeoRL, 344, L08201
Ma, Y. J., Russell, C. T., Fang, X., et al. 2015, GeoRL, 42, 9113
Matsunaga, K., Seki, K., Brain, D. A., et al. 2017, JGRA, 122, 9723
Matta, M., Mendillo, M., Withers, P., & Morgan, D. 2015, JGRA, 120, 766
McFadden, J. P., Kortmann, O., Curtis, D., et al. 2015, SSRv, 195, 199
Mitchell, D. L., Lin, R. P., Mazelle, C., et al. 2001, JGR, 106, 23419
Moore, T. E., & Horwitz, J. L. 2007, RvGeo, 45, RG3002
Ness, N. F., Acuña, M. H., Connerney, J. E. P., et al. 2000, JGR, 105, 15991
Nilsson, H., Carlsson, E., Gunell, H., et al. 2006, SSRv, 126, 355
Nilsson, H., Edberg, N. J. T., Stenberg, G., et al. 2011, Icar, 215, 475
Niu, D. D., Cui, J., Gu, H., et al. 2020, JGRA, 125, e27670
Ramstad, R., Barabash, S., Futaana, Y., Nilsson, H., & Holmström, M. 2016, GeoRL, 43, 10574
Russell, C. T., Luhmann, J. G., Schwingenschuh, K., Riedler, W., & Yeroshenko, Y. 1990, GeoRL, 17, 897
Weber, T., Brain, D., Mitchell, D., et al. 2019, GeoRL, 46, 2347
Wei, Y., Dubinin, E., Woch, J., et al. 2012, JGRA, 117, A03208
Withers, P., Flynn, C. L., Vogt, M. F., et al. 2019, JGRA, 124, 3100
Withers, P., Mendillo, M., Rishbeth, H., Hinson, D. P., & Arkani-Hamed, J. 2005, GeoRL, 32, L16204
Wu, X.-S., Cui, J., Xu, S. S., et al. 2019, JGRE, 124, 734
Xu, S., Mitchell, D., Liemohn, M., et al. 2017, JGRA, 122, 1831